

DOI: <http://doi.org/10.52716/jprs.v14i3.887>

## Thermal Maturity Map Based on Vitrinite Reflectance of Yamama Formation in Basrah Oil Fields, South of Iraq

Amna M. Handhal\*, Alaa M. Al-Abadi

<sup>1</sup>Department of Geology, College of Science, University of Basrah, Basrah, Iraq

\*Corresponding Author E-mail: [amna.handhal@uobasrah.edu.iq](mailto:amna.handhal@uobasrah.edu.iq)

Received 31/12/2023, Revised 21/02/2024, Accepted 25/02/2024, Published 22/09/2024



This work is licensed under a [Creative Commons Attribution 4.0 International License](https://creativecommons.org/licenses/by/4.0/).

### Abstract

This study aims to create a detailed thermal maturity map based on vitrinite reflectance in the Basrah oil fields in southern Iraq. The specific objective was to determine areas with the highest thermal maturity within the Yamama Formation. The selected fields for analysis were WQ-60, Lu-12, Zb-42, Nr-12, Mj-12, and Ru-72, which belong to the West Qurna, Luhas, Zubair, Nahr Umar, Majnoon, and Rumaila oilfields, respectively. The Petromod 1D software was used for basin modeling and thermal history reconstruction. By inputting geological and geophysical data, the software enabled the construction of a comprehensive thermal basin history. The primary focus was on evaluating vitrinite reflectance values, which serve as a proxy for thermal maturity. The results of the study revealed significant variations in thermal maturity within the Yamama Formation across the selected fields. The Nahr Umar field (Nr-12) exhibited the highest thermal maturity, characterized by elevated vitrinite reflectance values. This indicates that organic matter within the Yamama Formation has undergone significant heating and maturation processes in this particular field. On the other hand, the Zubair field (Zb-12) displayed the lowest vitrinite reflectance values, suggesting a lower level of thermal maturity. This could be attributed to different burial histories, variations in the thermal gradient, or other tectonic movements in the area.

**Keywords:** Introduction, Theory, Burial history, Thermal history, Vitrinite Reflectance.

**بناء خريطة النضوج الحراري اعتمادا على قيم انعكاس الفيترينيت لحقول النفط في البصرة، جنوب العراق**

### الخلاصة:

تهدف هذه الدراسة إلى إنشاء خريطة نضوج حراري مفصلة تعتمد على انعكاس الفيترينيت في حقول نفط البصرة في جنوب العراق. كان الهدف المحدد هو تحديد المناطق ذات النضج الحراري الأعلى في تكوين اليمامة. اختيرت الابار: WQ-60 و Lu-12 و Zb-42 و NR-12 و Mj-12 و Ru-72، التي تنتمي إلى حقول نفط غرب القرنة واللحيس والزبير ونهر عمر ومجنون والرميلة، على التوالي. تم استخدام برنامج Petromod 1D لنمذجة الأحواض وإعادة بناء التاريخ الحراري للحوض. من خلال إدخال البيانات الجيولوجية والجيوفيزيائية، حيث تم إنشاء تاريخ حراري شامل للحوض. كان التركيز الأساسي على

تقييم قيم انعكاس الفيترينيت، والتي تعمل كمؤشر للنضج الحراري ومن ثم رسم خريطة توزيع النضوج الحراري لحقول محافظة البصرة. أظهرت نتائج الدراسة وجود اختلافات معنوية في النضج الحراري ضمن تكوين اليمامة عبر الحقول المختارة. حيث أظهر حقل نهر عمر (NR-12) أعلى نضج حراري، ويتميز بارتفاع قيم انعكاس الفيترينيت. يشير هذا إلى أن المادة العضوية في تكوين اليمامة قد خضعت لعمليات تسخين ونضج كبيرة في هذا الحقل بالذات. من ناحية أخرى، أظهر حقل الزبير (Zb-12) أقل قيم انعكاس للفيترينيت، مما يشير إلى مستوى أقل من النضج الحراري. يمكن أن يُعزى ذلك إلى تواريخ الدفن المختلفة، أو الاختلافات في التدرج الحراري، أو الحركات التكتونية الأخرى في المنطقة.

## 1. Introduction:

Oil is present in various reservoir rocks of different ages. Over geological time, significant amounts of organic materials have accumulated due to Iraq's location along the ancient Tethys Sea basin axis. This led to high marine organic production because of the presence of strong upwelling currents, along with the confinement of the Tethys Sea currents parallel to the equator. These conditions created reduced marine environments that preserved organic materials beneath the accumulation of numerous sediments in the region. Thick cap rock formations were subsequently developed above these sediments, facilitated by the repeated advance and retreat of the sea during that period [1].

The unique occurrence of structural and stratigraphic oil traps results from Iraq's alignment with the Zagros mountain-building process. As a consequence of these tectonic activities, the oils formed from those organic materials settled in the current reservoir rocks, making them among the largest oil fields globally [2].

The term "petroleum system" encompasses all geological elements and processes that contributed to the existence of oil and gas in current traps [3]. The primary elements include source rocks, migration paths, reservoir rocks, seals, traps, and the geological processes that led to the formation of these elements. Several petroleum systems exist, including those focused on the relationship between source rocks and oil accumulations [4]. Basin modeling, burial history, maturity, and biomarker applications also play crucial roles. The burial history of a sedimentary basin is a fundamental factor in reconstructing and comprehending its evolution. Additionally, numerical modeling techniques are employed to determine burial history in sedimentary basins (e.g., [5]). Therefore, a prerequisite for a comprehensive understanding of geology is familiarity with rock properties, stratigraphic positioning, and thickness. The Cretaceous period is considered a crucial geological epoch in Iraq and the broader Middle East region due to its significant reservoir and hydrocarbon-forming formations. Among these formations is the Yamama Formation, which ranges in age from L. Berrisian to Valangian. This formation exhibits all the essential prerequisites

for a robust petroleum system, including well-developed mature source rocks, effective reservoir rocks for hydrocarbon retention. The Yamama Formation holds significance due to its substantial reservoir units located in central and southern Iraq, along with the concurrent presence of source rock intervals, [6].

In order to investigate the spatial distribution of thermal maturity, six oil fields were selected in Basra Governorate, namely Zubair, West Qurna, Nahr Umar, Majnoon, Luhais, and Rumaila. The study area is situated within the Zubair subzone in the Mesopotamian Basin, Figure (1). The Yamama Formation, which was deposited during the Lower Cretaceous period, is found stratigraphically between the Ratawi Formation of Valanginian-Hauterivian age, which overlies it, and the Suliay Formation of Tithonian-Berriasian age, which underlies it. The contact boundaries between these formations are gradual and correlated, as described by [7] (Figure 2). According to [8], the upper contact of the Yamama Formation with the Ratawi Formation is a conformable boundary, marked by the appearance of clean limestone rocks overlain by the marly limestone rocks of the Ratawi Formation. The lower contact of the Yamama Formation with the Suliay Formation is determined by the appearance of marly limestone rocks, which characterize the clay-rich feature of the Suliay Formation. The Yamama Formation is divided into three main lithological rock units: the lower unit is composed of porous and permeable bioclastic limestone rocks at the base of the formation, the middle part consists of compact limestone rocks, and the uppermost part represents fissured limestone with high porosity and permeability.

The primary aim of this study is to identify the most favorable regions for hydrocarbon generation, create maps depicting the distribution of thermal maturity, and subsequently pinpoint areas of hydrocarbon accumulation and migration within the fields located in Basra Governorate.

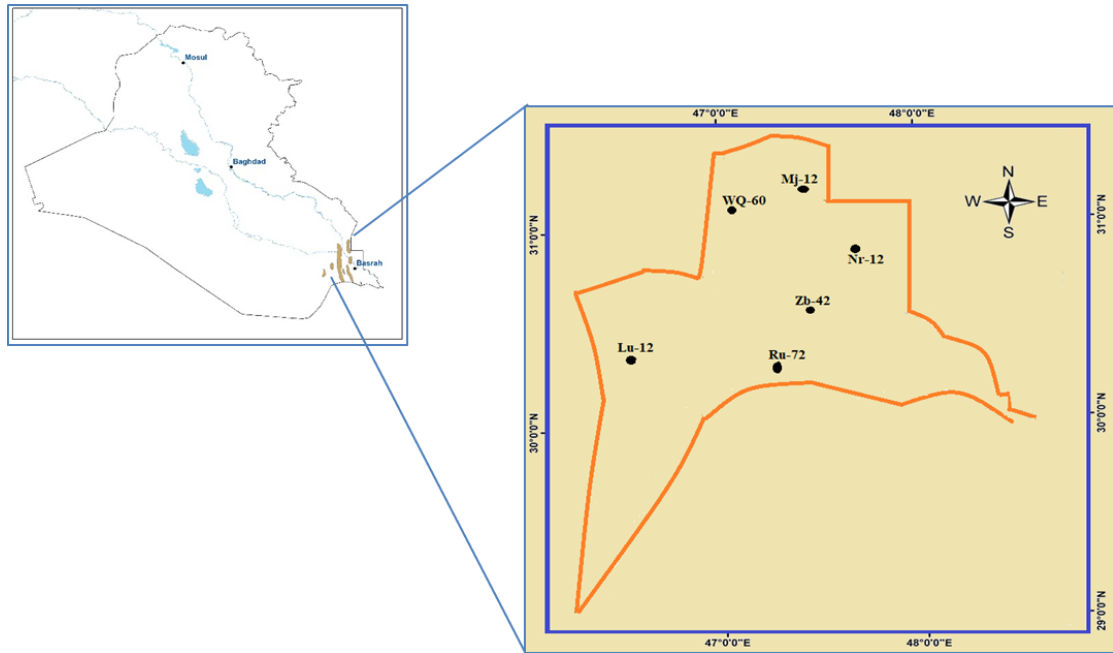


Fig. (1): The location of the study area

Age	Formation	Lithology	Lithology Description
L. Miocene-Recent	Dibdibba		Sand & pebble
E-M. Miocene	Fatha (Lower Fars)		Clay, Silt, Marl or Limestone
	Ghar		Sandstone (clay rich)
M-L.Eocene	Dammam		Dolomite, porous vuggy
Paleocene- E. Eocene	Rus		Anhydrite, Interbedded with Dolomite. Cap Rx.
	Umm-Er-Radhuma		Dolomite with Anhydrite
Late Cretaceous	Tayarat		Shale at top, Dolomite, grey
	Shiranish		Limestone marly
	Hartha		Limestone interbedded with Dolomite
	Sadi		Limestone white chalky
Middle Cretaceous	Tanuma		Shale. Cap Rx.
	Khasib		Argillaceous Chalky Limestone with shale
	Mishrif		Limestone. Reservoir Rx
	Ahmadi		Shale & Limestone interbeds
Early Cretaceous	Mauddud		Limestone
	Nahr Umr		Shale interbedded with sandstone
	Shuaiba		Limestone and dolomite
Late Jurassic	Zubair		Shale and sandstone. Reservoir Rx
	Ratawi		Shale interbedded with limestone
	Yamama		Limestone. Reservoir Rx
Middle Jurassic	Sulayy		Limestone, argillaceous and marly
	Gotnia		Anhydrite. Cap Rx.
	Najmah		Limestone interbedded with Shale
Middle Jurassic	Sargelu		Limestone interbedded with Shale. Source Rx.

**Legend Title**

- Anhydrite
- Dolomite
- Limestolom
- Limestarly
- Limesthaly
- Limestone
- Marl
- Sandstone
- Shale
- Shale & Sand
- Shale&Lime

Fig. (2): Stratigraphy column of the study area.

## **2. Material and Methods**

The burial history and thermal maturity of Six oil fields were modeled in one dimension using PetroMod 1D. PetroMod is a widely used software tool in the petroleum industry for modeling and simulating the thermal and geological evolution of sedimentary basins and hydrocarbon systems. It helps in understanding the generation, migration, and accumulation of hydrocarbons over geological time scales. In the context of PetroMod 1D, you're likely referring to 1D basin modeling, which focuses on the vertical evolution of a single geological column.

Here's a basic outline of the steps involved in performing a 1D basin modeling study using PetroMod:

### **2.1 Data Input and Geological Model Setup:**

- Define the stratigraphy of the basin, including rock layers, lithology, and thicknesses.
- Input paleo-temperature and paleo-burial data for each layer based on well data or regional knowledge.
- Specify the heat flow and thermal properties for the basin.

### **2.2 Generation and Expulsion Modeling:**

- Input the organic matter type, quantity, and thermal properties.
- Define the kinetics of hydrocarbon generation and expulsion based on source rock properties.
- Model the transformation of organic matter to hydrocarbons and the timing of expulsion.

### **2.3 Migration and Accumulation Modeling:**

- Specify migration pathways and migration efficiency factors.
- Simulate the migration of hydrocarbons through the geological layers.
- Model the accumulation of hydrocarbons in traps, based on structural and stratigraphic elements.

### **2.4 Temperature and Maturation Modeling:**

- Simulate the evolution of temperature over time due to heat flow and burial history.
- Calculate the thermal maturity of organic matter, indicating the level of hydrocarbon generation.

**Table (1): The Lu-12 well data input encompasses information on chronostratigraphic units, formation tops, and the ages of depositional and erosional events within the study area.**

Layer	Top (m)	Base (m)	Thick (m)	Eroded (m)	Depo from(Ma)	Depo to (Ma)	Eroded from(Ma)	Eroded to (Ma)	Lithology
Dibdibba Lower	0	54	54	52	10.2	5	5	0	SANDcongl
Fares	54	144	90		16.5	10.2			LIMEarly
Ghar	144	248	104		23	16.5			SANDcongl
Dammam	248	468	220	405	45	36.5	36.5	23	LIMEdolom
Rus	468	645	176		53	45			LIME&EVAP
Umm Er Radhuma	645	1103	458		62.3	53			LIME&EVAP
Tayarat	1103	1375	272	319	68.2	65	65	62.3	LIME&EVAP
Shiranish	1375	1478	103		70.4	68.2			LIMEarly
Hartha	1478	1759	281		80	70.4			LIMESTONE
Sadi	1759	2006	247		86	80			LIMESTONE
Tanuma	2006	2060	54		87	86			SHALE
Khasib	2060	2095	34		89	87			LIMESTONE
Mishrif	2095	2213	118	77	92	90	90	89	LIMESTONE
Rumaila	2213	2290	78		93	92			LIMeshaly
Ahmadi	2290	2408	117		94	93			SHALE&LIME
Mauddud Naher	2408	2494	86		95	94			LIMESTONE
Umr	2494	2725	231		107	95			SAND&SHALE
Shuaiba	2725	2785	60		112	107			LIMESTONE
Zubair	2785	3330	545		118	112			SAND&SHALE
Ratawi	3330	3608	278		125	118			SHALE&LIME
Yamama	3608	3770	162		135	125			LIMEdolom
Sulaiy	3770	4021	250		140	135			LIMeshaly

### 2.5 Fluid Properties and Phase Behavior:

- Calculate the properties of generated hydrocarbons, such as composition and phase behavior.
- Determine the type of hydrocarbons (oil, gas) generated based on maturity and source rock properties.

### 3. Theory and Calculation

A one-dimensional approach was employed to model the burial history and thermal maturity of four oil fields utilizing PetroMod 1D. PetroMod 1D is a comprehensive software package that seamlessly combines seismic and geological interpretations with multi-dimensional simulations of

thermal 3-phase fluid and petroleum migration histories within sedimentary basins. This software integrates various processes including deposition, pore pressure calculations, compaction, heat flow analysis, temperature determination, calibration parameter kinetics, hydrocarbon generation modeling, adsorption and expulsion processes, fluid analysis, and migration [9]. The software requires substantial input data, encompassing the following aspects:

1. Deposition: The upper layer's surface is established during sedimentation or eroded through erosion processes. Identification of deposition events and hiatus allows determination of paleo-deposition times for layers. New bed calculation involves porosity-controlled backstripping using current thickness or structural restoration programs [10].
2. Porosity Determination: Porosity diminishes due to compaction during burial. Various methods exist for porosity calculation, with open hole well logs like sonic, neutron, and density logs being optimal. These logs are plotted against depth to deduce compaction. Porosity-depth relationship follows an exponential formula [11]:

Where:

$$\phi_p = \phi_o e^{-cZ} \quad (1)$$

$\phi_p$ : Porosity at depth Z

$\phi_o$ : Initial porosity (0.49 for Sandstone, 0.55 for Shale, 0.52 for Limestone, 0.42 for Dolomite)

c: Coefficient (slope of porosity-depth curve, 0.0003 for Sandstone, 0.0005 for Shale, 0.0006 for Limestone, 0.0004 for Dolomite)

3. Sediment Decompaction: Backstripping starts by reconstructing the original sediment thickness ( $T_o$ ) of growing sedimentary fill up to current stratigraphic boundaries using present porosity ( $\phi_p$ ) and present thickness ( $T_p$ ). The equation is as follows [12]:

$$T_o = \frac{(1 - \phi_p)}{(1 - \phi_o)} \cdot T_p \quad (2)$$

4. Eroded Thickness: The PetroMod software employs the following equation to determine eroded thickness as input data [13]:

$$Eroded\ thickness = T_o * \frac{age\ of\ erosion}{age\ of\ deposition} \quad (3)$$

Where:  $T_o$ : Original sediment thickness

Heat Flow: Heat transfer in sediments involves conduction and radiation. Boundary conditions for heat flow analysis include sediment-water-interface temperature and basal heat flow. Mechanical and thermal crustal processes determine heat flow at the sediment base [10]. Heat flow calculation involves the following equation [14]:

$$Q_z = k \frac{dt}{dz} \quad (4)$$

where:  $Q_z$ : vertical component of heat flow ( $\text{MW} \cdot \text{m}^{-1}$ ),  $k$ : thermal conductivity ( $\text{W} \cdot \text{m}^{-1} \cdot ^\circ\text{C}^{-1}$ ),  $\frac{dt}{dz}$ : geothermal gradient ( $^\circ\text{C}/\text{km}$ ). Thermal conductivity calculation employs this equation [15]:

$$k = k_m^{(1-\phi)} * k_w^\phi \quad (5)$$

where:

$k$ : bulk thermal conductivity,  $k_w$ : water conductivity ( $0.59 \text{ W} \cdot \text{m}^{-1} \cdot ^\circ\text{C}^{-1}$ ),  $\phi$ : porosity (%) (calculate from well logs),  $k_m$ : rock matrix conductivity (1.45 for shale, 3.75 for dolomite, 2.64 for sandstone, 2.56 for limestone, 5.4 for anhydrite). The heat flow calculations involve deriving porosity from well logs, obtaining  $k_m$  values from lithological sections, and estimating the geothermal gradient from well log records (Ts, TD, BHT). Post PetroMod software execution, numerous petroleum system evaluation results are obtained, including thermal conductivity, porosity, heat flow, various pressure types, burial and thermal histories, and vitrinite reflectance.

#### 4. Results and Discussion

The burial history of the sedimentary basin is the key factor for reconstructing and understanding the basin's evolution. Additionally, numerical modeling techniques are used to determine the burial history in sedimentary basins (e.g., [5]). Therefore, a prerequisite for a thorough understanding of the geology, including knowledge of rock properties, stratigraphy, and thickness, is essential. Below is a summary of some results:

**4.1 Burial History:** The geological history is analyzed using numerical techniques to calculate the sediment accumulation rate and subsidence or uplift of the sedimentary basin over geological time. This analysis reveals the development and interpretation of geological events. The sedimentary basin consists of various rock layers deposited during different



geological time periods [16]. Subsidence curves and burial history for the studied wells (Figures 3) indicate the following periods:

A. Rapid to very rapid deposition periods include:

- Lower Cretaceous, encompassing: Yammama, Ratawi, and Zubair formations.
- Upper Cretaceous, including Mishrif Formation.
- Miocene-Oligocene, with Hartha & Ghar, Fatha & Ingana formations.

B. Moderate deposition periods include:

- Upper Cretaceous, comprising Shuaiba Formation.
- Eocene-Oligocene, involving Dammam Formation.

C. Slow deposition periods include:

- Nahr Umr Formation.
- Miocene, containing Um Radhum, Tanuma, and Khasib formations.

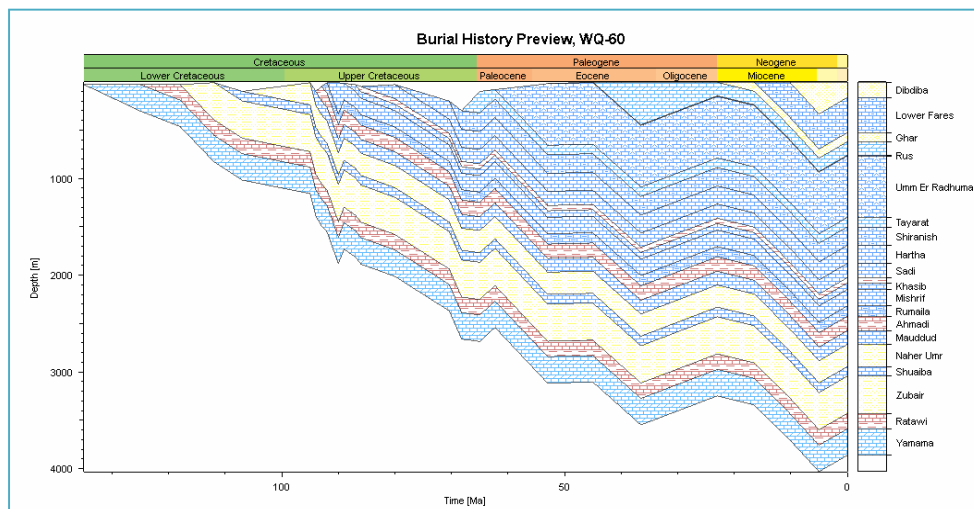


**Fig. (3): Burial History of WQ-60**

**4.2 Thermal History:** Burial history and thermal history can be utilized to determine the potential of oil and gas in sedimentary basins and estimate reservoir porosity. Furthermore, burial history curves from multiple locations can be employed to create paleo-structural maps at specific time intervals, in addition to thermal maturity information. This can serve as a tool to understand the timing of oil migration and potential migration pathways, correlated with the evolution of suitable traps. The timing of maximum temperature and maximum burial depth holds significant importance for the petroleum system within the study area. For most existing wells, the Paleocene to

Miocene era is characterized by periods of elevated temperatures due to increased deep burial, coupled with associated tectonic processes, as illustrated in Figure (4).

**4.3 Vitrinite Reflectance (R<sub>0</sub>):** Vitrinite reflectance stands as the most extensively employed indicator for gauging the maturity of organic materials [11]. This optical parameter is denoted as VR or R<sub>0</sub>, which signifies reflectance in oil. Vitrinite is a product of coalification originating from humic substances, itself derived from the lignin and cellulose present in plant cell walls [17]. The reflectance of the vitrinite maceral group appears to exhibit a smooth and predictable variation in relation to temperature ([18]; [19]).

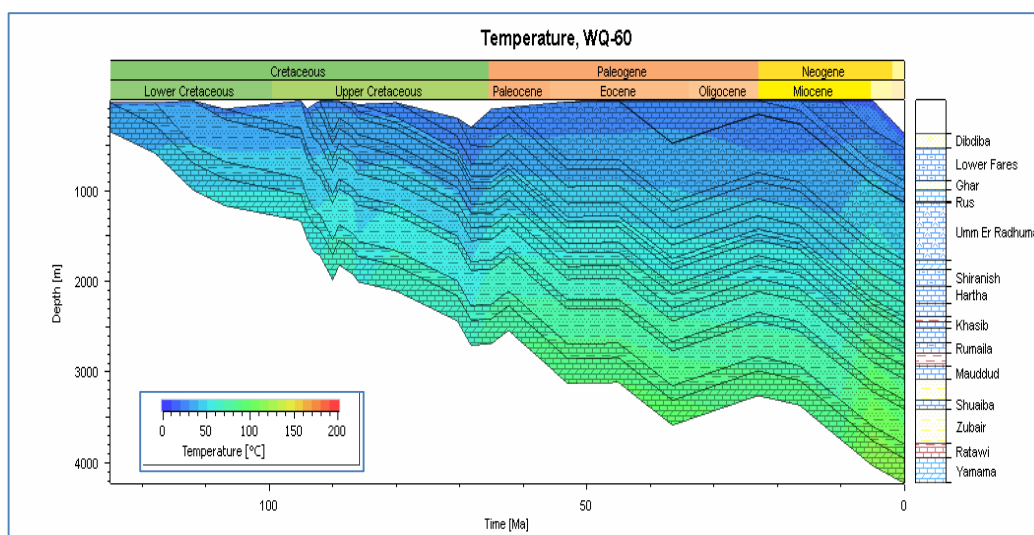


**Fig. (4): Thermal History of WQ-60.**

Notably, reflectance measurements taken from maceral types other than vitrinite (particularly in lacustrine sedimentary macerals), and even within different macerals within the vitrinite group, may exhibit significant differences [20]. [19] proposed a simplified model of R<sub>0</sub> based on chemical kinetics to account for changes in vitrinite composition over time and temperature. This model, named Easy %R<sub>0</sub>, employs an Arrhenius first-order parallel reaction approach with a distribution of activation energies. Easy %R<sub>0</sub> values are elucidated in Table (2) based on [19]. Models from [19] incorporate distributions of activation energies for four reactions: the elimination of water, carbon dioxide, methane, and higher hydrocarbons. The R<sub>0</sub> value is calculated using the Transformation Ratio (TR) for each reaction ( $R_0 = 0.45 + 1.15 * TR$ ). The thermal and burial histories were calibrated by comparing measured and calculated vitrinite reflectance data. The

kinetic EASY% Ro algorithm [19] was employed for calculating vitrinite reflectance. In the study area, vitrinite reflectance values are presented in Figure (5) and Table (3).

**Table (2): Easy vitrinite reflectance after [19].**

0.25 – 0.55	Immature
0.55 – 0.70	Early oil
0.70 – 1.00	Main oil
1.00 – 1.30	Late oil
1.30 – 2.00	Wet gas
2.00 – 4.00	Dry gas
> 4.0	Over mature

**Table (3): The values of the vitrinite reflectance of the wells of the study area**

Well No.	Formation	Ro %	Stage
WQ-60	Yamama	0.72	Main Oil
Lu-12	Yamama	0.68	Early Oil
Zb-42	Yamama	0.67	Early Oil
NR-12	Yamama	1	Late Oil
Mj-12	Yamama	0.88	Main Oil
Ru-72	Yamama	0.77	Main Oil

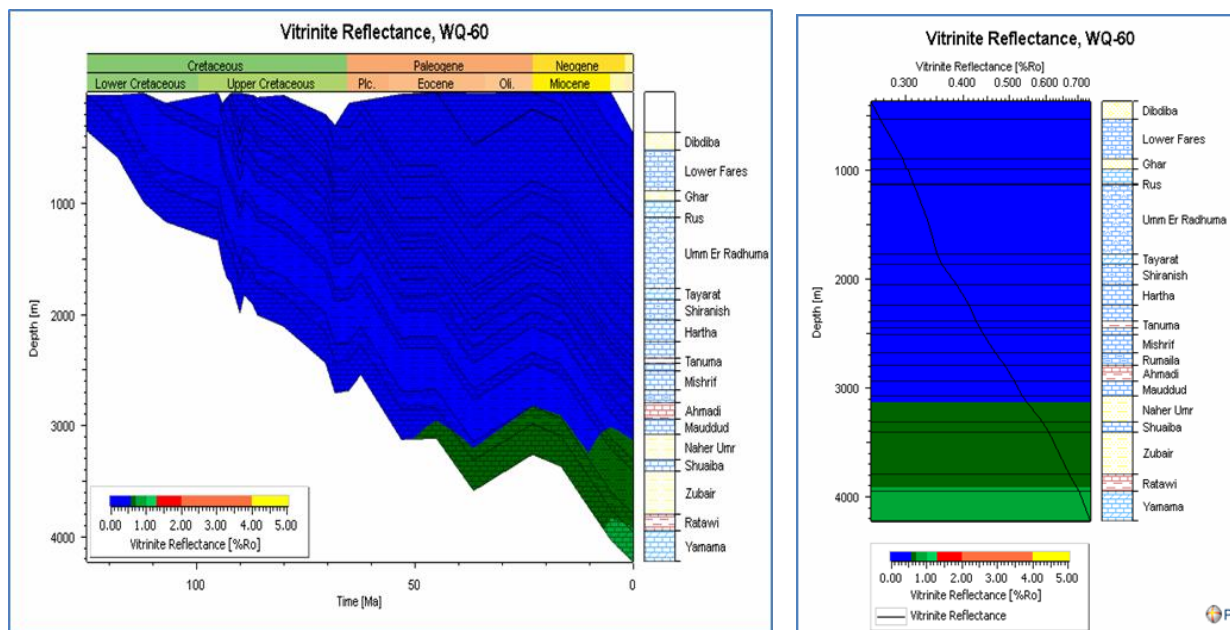


**Fig. (5): Distribution of vitrinite reflectance with burial history and depth.**

Delving deeper into the dataset presented in Table (3) and analyzing the information depicted in Figures (5) and (6), a captivating narrative unfolds regarding the thermal maturity dynamics within the Yammama Formation of the Nr-12 Nahr Umr area. The thermal maturity gradient between the two wells, Nr-12 and Zb-42, stands as a testament to the diverse thermal histories that these formations have undergone. In Nr-12, situated along the Nuhr Umr, the Yammama Formation has experienced an extensive journey of thermal transformation, leading it to the advanced "Late Oil" stage. The remarkably high  $R_0$  value of 1 reflects the substantial maturation processes that have taken place. This suggests that the organic materials have been subjected to prolonged exposure to elevated temperatures, resulting in significant hydrocarbon generation potential. In contrast, the Yammama Formation in Zb-42 Zubair Well portrays a different thermal story. With an  $R_0$  value of 0.68, this formation is situated within the "Early Oil" phase. This disparity in thermal maturity implies that the organic constituents have undergone comparatively milder thermal alteration in this region. This observation could be indicative of distinct geological conditions that governed the temperature history of the organic materials.

Analyzing the broader thermal maturity distribution across the region, a thermal maturity map visually highlights varying levels of maturity across the Basra Governorate. The northern sector of the governorate emerges as a hotspot of heightened thermal maturity. The prevalent conditions in this region have contributed to subjecting the organic materials to prolonged elevated temperatures, fostering advanced thermal transformation. The interplay of geological factors, possibly tectonic and structural activities, might have played a role in shaping this elevated thermal history. Conversely, the eastern and southeastern parts of the governorate exhibit relatively subdued thermal maturity levels. This divergence in thermal exposure could be attributed to geological factors that have shielded the organic constituents from prolonged high-temperature conditions. This area might have experienced a different tectonic and thermal evolution, resulting in a distinct thermal maturity trend.

In conclusion, the comprehensive analysis of Table (2) and Figures (5) and (6) paints a detailed portrait of the intricate thermal maturity variations within the Yammama Formation. This narrative captures the geological intricacies that have driven the hydrocarbon generation potential in different regions of the Basra Governorate. The journey from "Late Oil" to "Early Oil" is a reflection of the diverse geological forces that have shaped the thermal history of these formations over geological epochs.

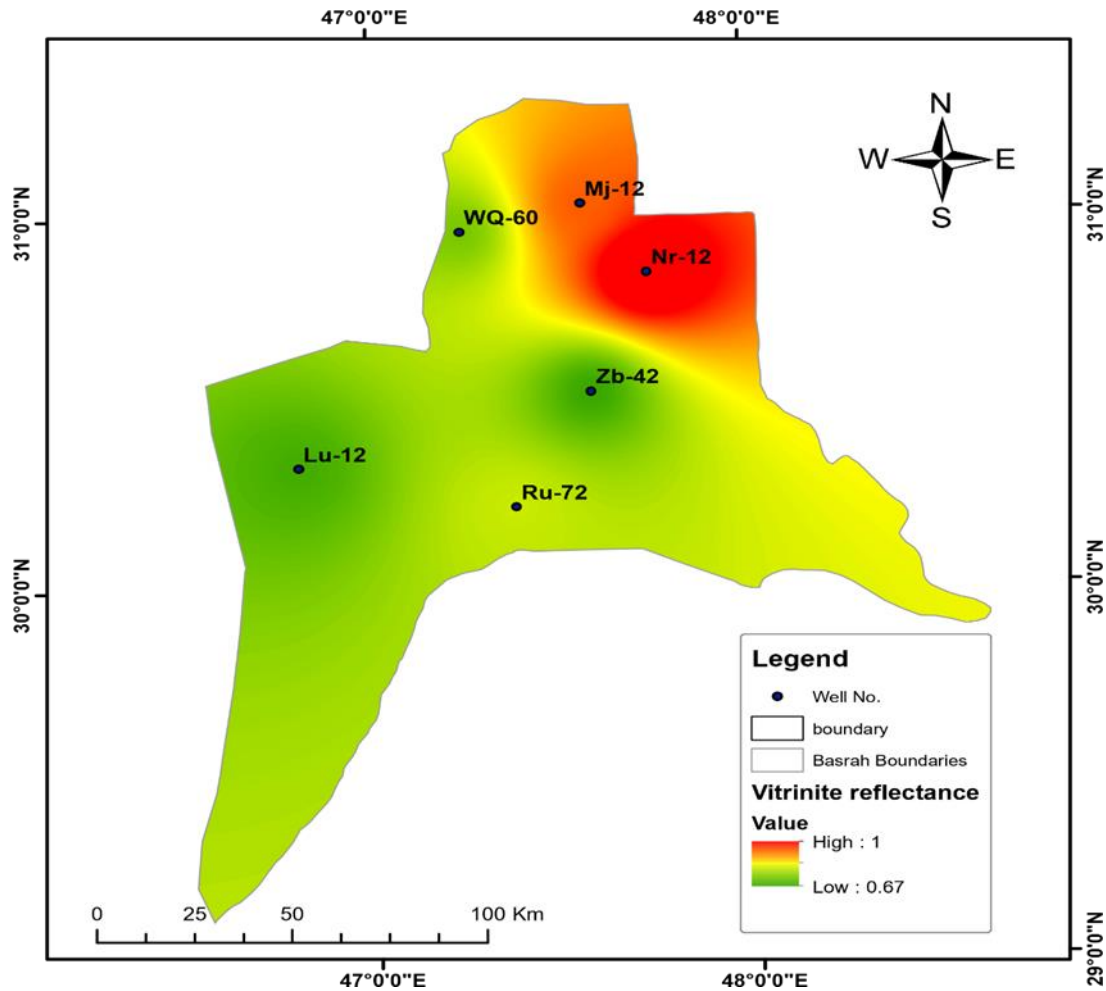


**Fig. (6):** A map of the southern Iraq fields illustrates the distribution of vitrinite reflectance values for the fields WQ-60, Lu-12, Zb-42, NR-12, Mj-12, and Ru-72.

## 5. Conclusions

1. The study area exhibits a distinct geological landscape characterized by the presence of diverse subsidence periods spanning various geological epochs. These intervals encompass rapid, moderate, and slow sediment deposition processes, playing a pivotal role in shaping the intricate stratigraphic evolution over geological time spans.
2. The thermal history of the basin unveils a remarkable aspect: a pronounced elevation in temperature regimes during the Miocene epoch. This thermal intensification is attributed to a confluence of factors, including the substantial burial depth attained by sedimentary layers and the simultaneous occurrence of tectonic activities that accompanied this specific geological era.

3. Vitrinite reflectance values exhibit a range spanning from 0.67 to 1. These values directly correspond to distinct thermal maturity stages within the hydrocarbon generation process. Specifically, this range represents the transition from the early oil stage to the main oil stage, encompassing the Early Oil and Main Oil phases.
4. When examining the the spatial distribution of thermal maturity, a clear pattern emerges. The highest levels of thermal maturity are concentrated in the northern region of the Basra Governorate, with prominent instances noted at the Majnoon and Nahr Omar fields (Mj-Nr). In contrast, as one moves towards the western and southwestern parts of the Basra Governorate, a gradual decrease in thermal maturity becomes apparent. Notably, this trend is particularly noticeable at the Luhais field (Lu).
5. In summary, these observations and findings provide a comprehensive overview of the geological and thermal dynamics within the study area. The complex interplay of subsidence periods, thermal history, vitrinite reflectance values, and geographical distributions all contribute to unraveling the intricate geological story of the region, offering valuable insights into the hydrocarbon potential and evolution within the Basra Governorate.

## References:

- [1] R. J. Murriss, “Middle East: stratigraphic evolution and oil habitat”, *AAPG Bulletin*, vol. 64, no. (5), pp. 597-618, 1980. <https://doi.org/10.1306/2F918A8B-16CE-11D7-8645000102C1865D>
- [2] A. E. M. Narin, and A. S. Al-Shahran, “Sedimentary basins and petroleum geology of the Middle East”, *Elsevier*, p 843, 1997.
- [3] J. M. Hunt, “Petroleum geochemistry and geology (textbook)”, *Petroleum Geochemistry and Geology (Textbook)*, (2nd Ed.), *WH Freeman Company*, 1995.
- [4] K. E. Peters, C. C. Walters, and J. M. Moldowan, “The Biomarker Guide”, *Cambridge University Press*, U.K, 2005.
- [5] B. Bruns, R. di Primio, U. Berner, and R. Littke, “Petroleum system evolution in the inverted Lower Saxony Basin, northwest Germany: a 3D basin modeling study”, *Geofluids*, vol. 13, no. 2, pp. 246-271, 2013. <https://doi.org/10.1111/gfl.12016>
- [6] A. J. Al-Khafaji, F. M. Al-Najm, R. Al-Refaia, F. Sadooni, M. Al-Owaidi, and H. Al-Sultan, “Source rock evaluation and petroleum generation of the Lower Cretaceous Yamama Formation: Its ability to contribute to generating and expelling petroleum to cretaceous reservoirs of the Mesopotamian Basin, Iraq”, *Journal of Petroleum Science and Engineering*, vol. 217, 110919, 2022. <https://doi.org/10.1016/j.petrol.2022.110919>
- [7] S. Z. Jassim, and J. C. Goff, “Geology of Iraq”, *Published by Dolin*, Prague and Moravian Museum, Brno, Czech Republic, 341 p, 2006.
- [8] A. A. Al-Siddiki, “Subsurface geology of southern Iraq. 10th Arab Petrol”, *Congre. Tripoli, Libya*, 47 p, 1977.
- [9] Schlumberger, User Guide petro Mode, 2011.
- [10] T. Hantschel, A. I. Kauerauf, “Fundamentals of basin and petroleum system modeling”, *Springer*, Berlin, p 476, 2009. <https://doi.org/10.1007/978-3-540-72318-9>
- [11] P. A. Allen, J. R. Allen, “Basin analysis: principles and applications”, *Blackwell*, Oxford, p 549, 2005.
- [12] A. M. Al-Matary, H. M. Ahmed, “Basin analysis study of block 10 in the Say’un-Masilah Basin, Yemen, using a 1D backstripping method”, *Arab J Geosci*, vol. 5, no. 3, pp. 529–554, 2011. <https://doi.org/10.1007/s12517-011-0280-0>

- [13] A. M. Handhal, and M. M. Mahdi, “Basin modeling analysis and organic maturation for selected wells from different oil fields, Southern Iraq”, *Modeling Earth Systems and Environment*, vol. 2, pp. 1-14, 2016. <https://doi.org/10.1007/s40808-016-0247-y>
- [14] T. H. Mccullogh, N. D. Nasser, “Thermal history of sedimentary basins; introduction and overview”, *Springer, New York, NY*, pp. 1–11, 1989. [https://doi.org/10.1007/978-1-4612-3492-0\\_1](https://doi.org/10.1007/978-1-4612-3492-0_1)
- [15] R. C. Selley, “Elements of petroleum geology”, *Gulf Professional Publishing*, 1998.
- [16] M. Wangen, “Physical principles of sedimentary basin analysis”, *Cambridge University Press, Cambridge*, p 527, 2010.
- [17] G. H. Taylor, M. Teichmuller, A. Davis, C. F. Diessel, R. Littke, and P. Robert, “Organic petrology”, *Gebruder Borntraeger, Berlin, Stuttgart*, p 704, 1998.
- [18] A. K. Burnham, and J. J. Sweeney, “A chemical kinetic model of vitrinite maturation and reflectance”, *Geochimica et Cosmochimica Acta*, vol. 53, no. 10, pp. 2649-2657, 1989. [https://doi.org/10.1016/0016-7037\(89\)90136-1](https://doi.org/10.1016/0016-7037(89)90136-1)
- [19] J. J. Sweeney, A. K. Burnham, “Evaluation of a simple model of vitrinite reflectance based on chemical kinetics”, *AAPG Bulletin*, vol. 74, no. 9, pp. 1559–1570, 1990. <https://doi.org/10.1306/0C9B251F-1710-11D7-8645000102C1865D>
- [20] D. F. Bensley, J. C. Crelling, “The inherent heterogeneity within the vitrinite maceral group”, *Fuel*, vol. 73, no. 8, 1994, pp. 1306-1316, 1994. [https://doi.org/10.1016/0016-2361\(94\)90306-9](https://doi.org/10.1016/0016-2361(94)90306-9)